Color confinement, chiral symmetry breaking, and catalytic effect induced by monopole and instanton creations

Masayasu Hasegawa

Bogoliubov Laboratory of Theoretical Physics,

Joint Institute for Nuclear Research, Dubna, Russia

5th October 2022

BLTP, JINR, Dubna, Moscow, Russia

References of this seminar

In this seminar, I will talk about the recent outcomes in the following papers:

[1] **M. Hasegawa**, *Monopole and instanton effects in QCD*, JHEP 09 (2020) 113, [arXiv: 1807.04808], (2022).

[2] **M. Hasegawa**, *Color confinement, chiral symmetry breaking, and catalytic effect induced by monopole and instanton creations*, Submitted to EPJC in March, [arXiv: 2203.11357], (2022). Open access data for this research are provided in [https://doi.org/10.6084/m9.figshare.20942866].

[3] **M. Hasegawa**, *Instanton effects on chiral symmetry breaking and hadron spectroscopy*, PoS (LATTICE2021) 397, [arXiv: 2201.00431], (2022).

Monopoles

- A single quark has never been observed experimentally.
- We still do not know why we cannot observe particles of a single-color charge.
- To explain this phenomenon, 'tHooft [Proceedings of EPS international (1976)] and Mandelstam [Phys.Rep 23, 245 (1976)] provided a convincing description that a magnetic monopole that condenses in the QCD vacuum causes the dual Meissner effect and that color charged particles are confined.
- A significant number of simulations have been conducted under lattice gauge theory, and sufficient results have been obtained that support this explanation.
- However, numerical results demonstrated a serious problem with gauge dependence [PRL 94 (2004) 132001].
- Therefore, Japanese research groups (Kanazawa University and Chiba University) study the monopole independent of the choice of gauge conditions.
- Kanazawa University started from the numerical simulation in SU(2) [PRD 77 (2008) 034502; 80 (2009) 054504].
- Chiba University tries to theoretically define the monopole in a gauge-invariance way [PRD 83 (2010) 114016].

Instantons

- The spontaneous breaking of chiral symmetry causes interesting phenomena in the low energy of QCD [Nambu and Goldstone].
- Once chiral symmetry spontaneously breaks, a massless pion, which is the NG (Nambu-Goldstone) boson, appears, and the chiral condensate, which is an order parameter of chiral symmetry breaking, obtains nonzero values.
- The quarks obtain small masses from the nonzero values of the chiral condensate.
- The pion decay constant is defined as the strength of the coupling constant between the NG boson and the axial-vector current.
- The pion obtains mass by supposing a partially conserved axial current (PCAC) [Weinberg].
- These phenomena are well explained by models concerning the instanton [Belavi, Dyakonov, and Shuryak].
- The models demonstrate that the chiral condensate and the pion decay constant are estimated from the instanton vacuum and that instantons induce the breaking of the chiral symmetry [Dyakonov].

Purpose of this research project

- In condensed matter physics, a research group has created Dirac monopoles in a Bose-Einstein condensate and detected the monopoles through their experiments [Nature 505 (2014) 657, Science 348 (2015) 544].
- In high-energy physics, the “Monopole and Exotics Detector at the LHC (MoEDAL)’’ has already operated [https://videos.cern.ch/record/1360998].
- This experiment aims to explore magnetic monopoles, dyons, and other highly ionizing particles in proton-proton collisions at the LHC.
- This detector has been upgraded to the "MoEDAL-Apparatus for Penetrating Particles (MoEDAL-APP) [https://home.cern/science/experiments/moedal-mapp].
- **Our research project aims to show the effects of magnetic monopoles and instantons on observables, which experiments can detect.**
- **Our final goal is to reveal the existence of magnetic monopoles and instantons in the real world.**
- **For these purposes, we first perform simulations in lattice gauge theory.**

Purpose of this research

- In our research, first, we add a pair of monopole and anti-monopole to the QCD vacuum of the quenched gauge field configurations in SU(3) by applying the monopole creation operator to the vacuum [Bonati, et al. (2012)].
- Second, to increase the number of monopoles and anti-monopoles in the QCD vacuum, we generate configurations varying the magnetic charges of the monopole and anti-monopole.
- Third, we calculate the low-lying eigenvalues and eigenvectors of the Dirac operator of the overlap fermions, which preserves the exact chiral symmetry in lattice gauge theory, using these configurations.
- Finally, we reveal the quantitative relations among monopoles, instantons, color confinement, and chiral symmetry breaking. Moreover, we confirm our outcomes by comparing numerical results with predictions.

Purpose of this research

- The main purpose of this study [2] is to **investigate the influences of finite lattice volume and discretization on our outcomes in [1].**
- We then obtain the **results at the continuum limit by interpolation.**
- To inspect these influences and to interpolate the outcomes, we generate many kinds of configurations from low to finite temperatures.

Our outcomes

We have already obtained the following outcomes [PRD 91 (2015) 054512, 1,3]**:**

(1) A monopole and anti-monopole pair makes an instanton or an anti-instanton.

(2) The additional monopoles and anti-monopoles do not affect the vacuum structure and add topological charges.

(3) The additional monopoles and anti-monopoles form the long monopole loops, which are closely related to the color confinement, and the length of the monopole loops lengthens with increasing the magnetic charges of the additional monopoles and anti-monopoles.

(4) The additional monopoles and anti-monopoles do not affect the spectra of the overlap Dirac operator and change only the scale of the distributions of the eigenvalues.

Our outcomes

(5) The renormalized chiral condensate in the $\overline{\mathrm{MS}}$-scheme at 2 [GeV] decreases in direct proportion to the square root of the number density of the instantons and anti-instantons.

(6) The renormalized average mass of up and down quarks and strange quark mass in the $\overline{\mathrm{MS}}$-scheme at 2 [GeV] become heavy in direct proportion to the square root of the number density of the instantons and anti-instantons.

(7) The masses and decay constants of pion and kaon increase in direct proportion to the one-fourth root of the number density of the instantons and anti-instantons.

(8) The decay width of the charged pion becomes wider than the experimental outcome by increasing the number density of the instantons and anti-instantons. This results in the lifetime of the charged pion becoming shorter than the experimental outcome. **This is the catalytic effect.**

(9) The masses of eta and eta-prime mesons become heavy by increasing the number density of the instantons and anti-instantons.

Simulation parameters of low temperatures ($L_s \leq L_t$)

- **We add a monopole and anti-monopole pair to gauge field configurations of quenched SU(3) of low temperatures (66~148 [MeV]).**
- **We generate the standard configurations and the configurations with the additional monopoles and anti-monopoles.**
- **To change the number of monopoles and anti-monopoles, we vary the magnetic charges.**
- The magnetic charges of the monopole m_c (positive) range from **0** to **5**.
- The magnetic charges of the anti-monopoles $-m_c$ (negative) range from **0** to **-5**.
- We add the same magnitude of the magnetic charges; thus, the total magnetic charge is zero.
- The magnetic charge m_c indicates that both charges are added.
- The electric charge **g** is added.

Simulation parameters of low temperatures ($L_s \leq L_t$)

A part of the list of configurations

- We set the value of the lattice spacing at β = 6.0000 for to investigate the influence of the finite lattice volume.

β	a [fm]	V	m_c	Nconf
5.8457	0.1242	$12^3 \times 24$	Normal conf, 0-5	$9 \times 10^2 \sim 1.1 \times 10^3$
5.9256	0.1065	$14^3 \times 28$	Normal conf, 0-5	$8 \times 10^2 \sim 9 \times 10^2$
6.0000	9.3150×10^{-2}	$14^3 \times 28$	Normal conf, 0-5	$1.7 \times 10^3 \sim 1.8 \times 10^3$
		$16^3 \times 32$	Normal conf, 0-5	$9 \times 10^2 \sim 1.0 \times 10^3$
6.0522	8.5274×10^{-2}	$18^3 \times 32$	Normal conf, 0-6	$8 \times 10^2 \sim 9 \times 10^2$
6.1366	7.4520×10^{-2}	$20^3 \times 40$	Normal conf, 4-5	$4 \times 10^2 \sim 5 \times 10^2$

Simulation parameters of low temperatures ($L_s \leq L_t$)

A part of the list of configurations

- We set the physical lattice volume at V_{phys} = 9.8582 [fm^4] and change the lattice volumes and values of the parameter β for to investigate the discretization influence on the results.
- We then interpolate the numerical results to the continuum limit.

β	a [fm]	V	m_c	Nconf
5.8457	0.1242	$12^3 \times 24$	Normal conf, 0-5	$9 \times 10^2 \sim 1.1 \times 10^3$
5.9256	0.1065	$14^3 \times 28$	Normal conf, 0-5	$8 \times 10^2 \sim 9 \times 10^2$
6.0000	9.3150×10^{-2}	$14^3 \times 28$	Normal conf, 0-5	$1.7 \times 10^3 \sim 1.8 \times 10^3$
		$16^3 \times 32$	Normal conf, 0-5	$9 \times 10^2 \sim 1.0 \times 10^3$
6.0522	8.5274×10^{-2}	$18^3 \times 32$	Normal conf, 0-6	$8 \times 10^2 \sim 9 \times 10^2$
6.1366	7.4520×10^{-2}	$20^3 \times 40$	Normal conf, 4-5	$4 \times 10^2 \sim 5 \times 10^2$

Simulation parameters of finite temperatures ($L_s > L_t$)

- **We add a monopole and anti-monopole pair to gauge field configurations of the quenched SU(3) of finite temperatures (245~477 [MeV]).**
- **We generate the standard configurations and the configurations with the additional monopoles and anti-monopoles.**
- The magnetic charges of the monopole **m_c** (positive) are **2, 4, 6,** and **8.**
- The magnetic charges of the anti-monopoles **$-m_c$** (negative) are **-2, -4, -6,** and **-8**.
- We add the same magnitude of the magnetic charges; thus the total magnetic charge is zero.
- The magnetic charge **m_c** indicates that both charges are added.
- The electric charge **g** is added.

Simulation parameters of finite temperatures ($L_s > L_t$)

- The critical temperature of the quenched SU(3) is obtained as follows [hep-lat: 0306005]:

$$T_c r_0 = 0.750(5)$$

- The critical temperature is (r_0 = 0.5 [fm])

$$T_c^{\mathrm{sta}} = 296(2)\ [\mathrm{MeV}].$$

- The temperature of the configurations is determined by the following equation:

$$T r_0 = \frac{1}{N_t\,(a/r_0)}.$$

- First, we determine the lattice volume **18^3X6** to be at the critical temperature, and then find the value of the lattice spacing. V_{phys} = 5.34 [fm^4]

T/T_c^{sta}	$V_s \times N_t$	β	a/r_0	$\mathrm{N_{conf}} \times 10^3$
0.8282	$14^3 \times 6$	5.8074	0.2684	6.0
0.9155	$16^3 \times 6$	5.8563	0.2428	4.0-6.0
1.0000	$18^3 \times 6$	5.9019	0.2223	6.0
1.0822	$20^3 \times 6$	5.9445	0.2054	6.0-7.2
1.1624	$22^3 \times 6$	5.9848	0.1912	4.0-7.0
1.2408	$24^3 \times 6$	6.0230	0.1791	3.0-7.4
1.3176	$26^3 \times 6$	6.0594	0.1687	4.0-6.0
1.3929	$28^3 \times 6$	6.0941	0.1596	4.0-6.0
1.4669	$30^3 \times 6$	6.1274	0.1515	3.0-6.0
1.5396	$32^3 \times 6$	6.1592	0.1444	3.0-6.0
1.6112	$34^3 \times 6$	6.1897	0.1380	3.0-4.0

Simulation parameters

- We calculate the low-lying eigenvalues and eigenvectors of the overlap Dirac operators using these configurations.
- We use the supercomputers and PC-clusters at the Research Center for Nuclear Physics (RCNP) at Osaka University and the Yukawa Institute at Kyoto University.
- We save the eigenvalues and eigenvectors in the storage elements of the Japan Lattice Data Grid (JLDG) at the RCNP at Osaka University.
- We calculate observables using these eigenvalues and eigenvectors.
- The details of the simulation parameters; the lattice volume, lattice spacing, number of configurations, etc. are listed in a paper and data tables in [2].

Numerical calculations

First, we generate the SU(3) normal configurations as follows:

- The action is the plaquette (Wilson) gauge action ***S***.
- The lattice spacing is calculated [NPB 622 (2002) 328].
- Sommer scale r_0 = 0.5 [fm].
- Standard Monte Carlo simulations in which the gauge links ***U*** are updated using the heat bath and overrelaxation methods.

- **Plaquette gauge action**

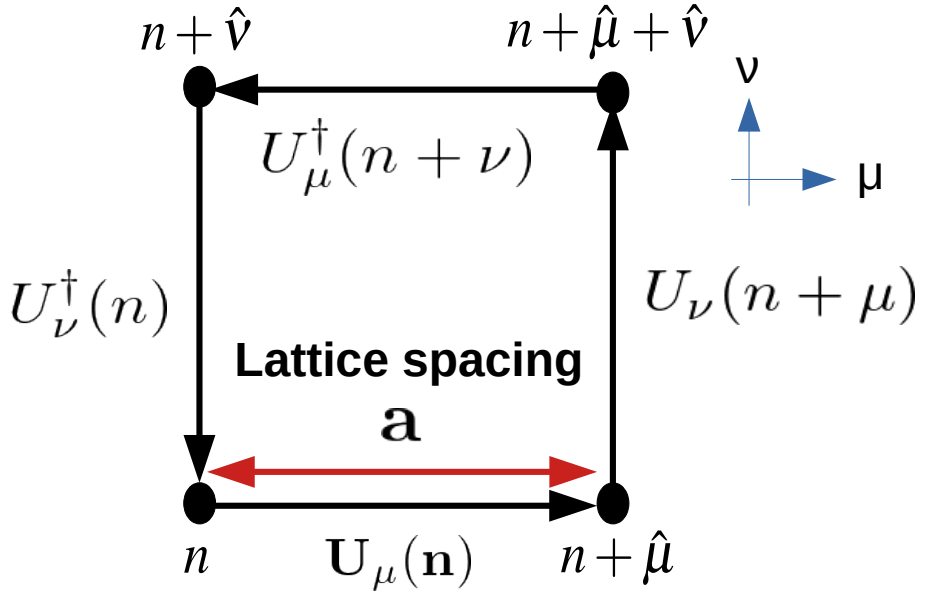

$$S = \sum_{n,\ \mu\neq\nu} \beta \mathrm{tr}[U_\mu(n)U_\nu(n+\mu)U_\mu^\dagger(n+\nu)U_\nu^\dagger(n)]$$

$$= 2\sum_{n,\ \mu<\nu} \beta \mathrm{Re tr}[U_{\mu\nu}(n)]$$

Monopole creation operator

Next, we create a pair of monopole and anti-monopole in QCD vacuum as follows:

- The monopole creation operator $\bar{\mu} = \exp\left(-\beta\overline{\Delta S}\right)$ acts on the vacuum.
- The plaquette action ***S*** is shifted as follows: $\mathbf{S} \to \mathbf{S} + \overline{\mathbf{\Delta S}}$
- A static Abelian monopole and anti-monopole pair is created [PRD 85 (2012) 065001].

- **The shifted plaquette action**

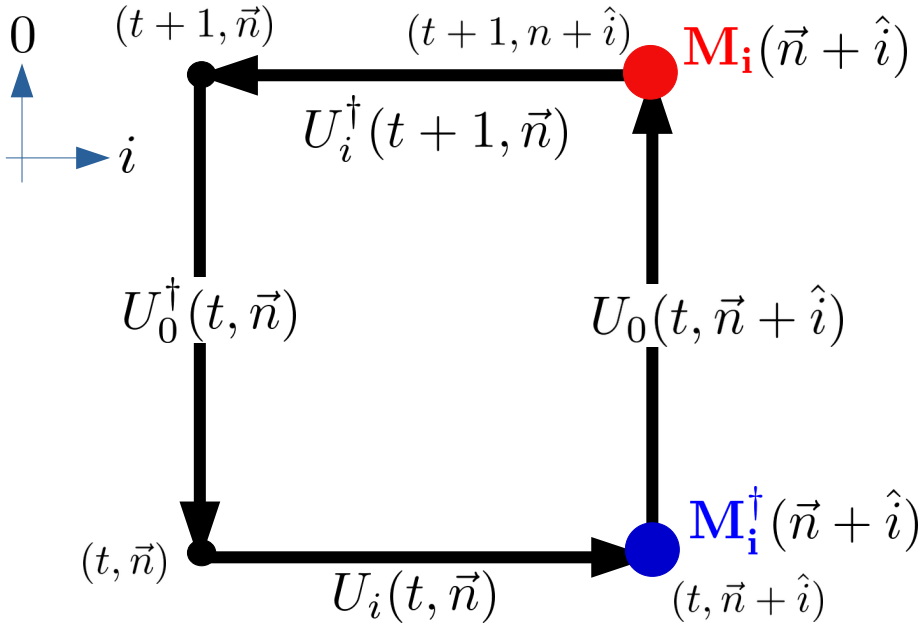

$$\mathbf{M_i}(\vec{n}) = \exp(iA_i^0(\vec{n}-\vec{x}_1))$$

$$\mathbf{M_i^\dagger}(\vec{n}) = \exp(-iA_i^0(\vec{n}-\vec{x}_2))$$

Monopole creation operator

- **Abelian monopole (Wu-Yang form)**

  [PRD 91 (2015) 054512]

$$\textbf{Monopole}: \mathbf{M_i}(\vec{n}) = \exp(iA_i^0(\vec{n} - \vec{x}_1))$$

$$\textbf{Anti-monopole}: \mathbf{M_i^\dagger}(\vec{n}) = \exp(-iA_i^0(\vec{n} - \vec{x}_2))$$

$(i)\ n_z - z \geqq 0$

$$\begin{pmatrix} A_x^0 \\ A_y^0 \\ A_z^0 \end{pmatrix} = \begin{pmatrix} \frac{\mathbf{m_c}}{2\mathbf{g}r} \frac{\sin\phi(1+\cos\theta)}{\sin\theta}\lambda_3 \\ -\frac{m_c}{2gr} \frac{\cos\phi(1+\cos\theta)}{\sin\theta}\lambda_3 \\ 0 \end{pmatrix}$$

$(ii)\ n_z - z < 0$

$$\begin{pmatrix} A_x^0 \\ A_y^0 \\ A_z^0 \end{pmatrix} = \begin{pmatrix} -\frac{m_c}{2gr} \frac{\sin\phi(1-\cos\theta)}{\sin\theta}\lambda_3 \\ \frac{m_c}{2gr} \frac{\cos\phi(1-\cos\theta)}{\sin\theta}\lambda_3 \\ 0 \end{pmatrix}$$

$$\mathbf{g} = \sqrt{\frac{6}{\beta}}: \ \text{(gauge coupling constant)}$$

- **Location of the monopole and anti-monopole**

$$D = |\vec{x}_1 - \vec{x}_2| \approx 1.1 \ [\text{fm}]$$

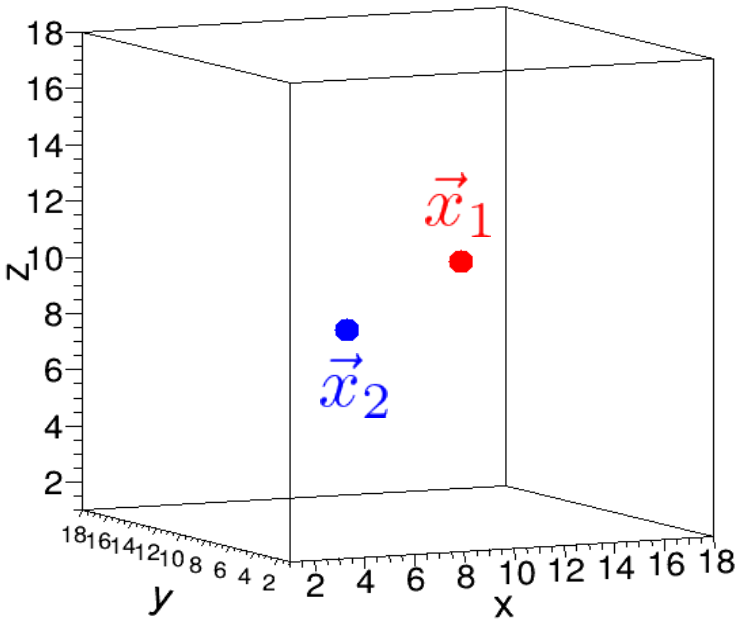

Monopole density

To confirm the additional monopole and anti-monopole, we compute the monopole densities.

- We diagonalize the SU(3) matrix under the condition of the **maximal Abelian gauge** and compute the density $\boldsymbol{\rho_m}$ of the monopole current $\boldsymbol{k_\mu}$, which satisfies the current conservation law $\nabla^*_\mu k^i_\mu(^*n) = 0$ [PRD 22 (1980) 2478].
- The current and density are as follows:

$$k^i_\mu(^*n) \equiv -\epsilon_{\mu\nu\rho\sigma}\nabla_\nu n^i_{\rho\sigma}(n+\hat{\mu}),\ \rho_m = \frac{1}{12V}\sum_{i,\mu}\sum_{^*n}|k^i_\mu(^*n)|/a^3\ [\mathrm{GeV}^3].$$

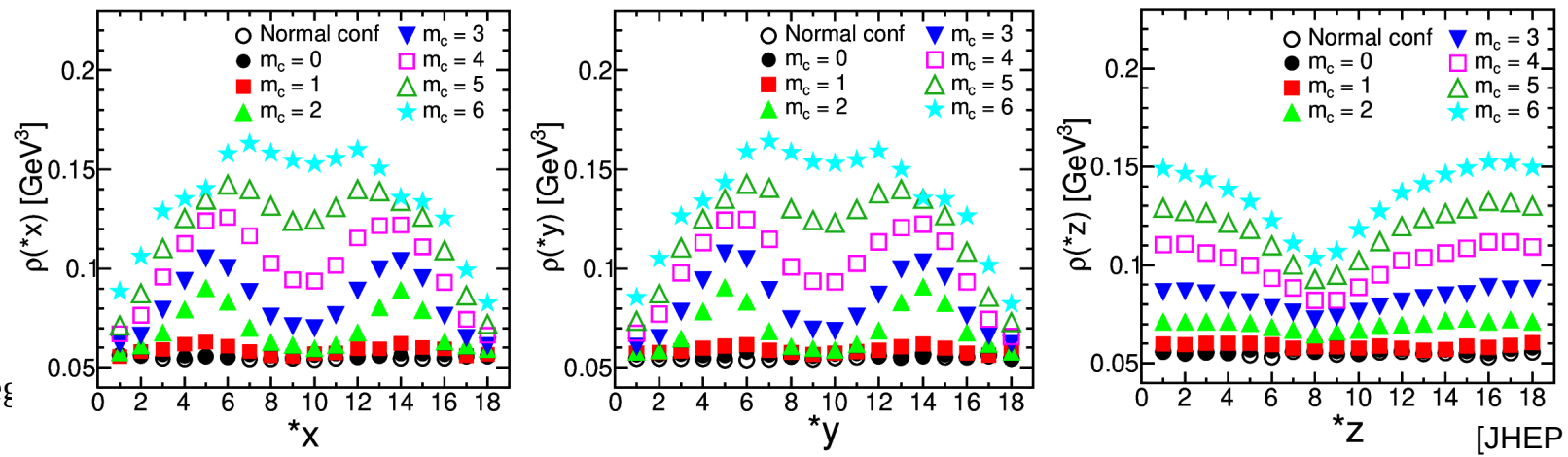

[JHEP 09 (2020) 131]

Number density of long monopole loops

- The monopole current satisfies the current conservation law. Therefore, the monopole currents form closed loops [NPB PS 34 (1994) 549].
- The monopole loops are classified into two clusters composed of long loops and short loops. The definition of the number density of the long monopole loops is as follows:

$$\rho_m^{long} \equiv \left(\frac{1}{12V} \sum_{i,\mu} \sum_{*n \in C} |k_\mu^i(*n)| \right)^{\frac{3}{4}} [\mathrm{GeV}^3]$$

- The longest monopole loop is closely related to color confinement.

[arXiv: 2203.11357]

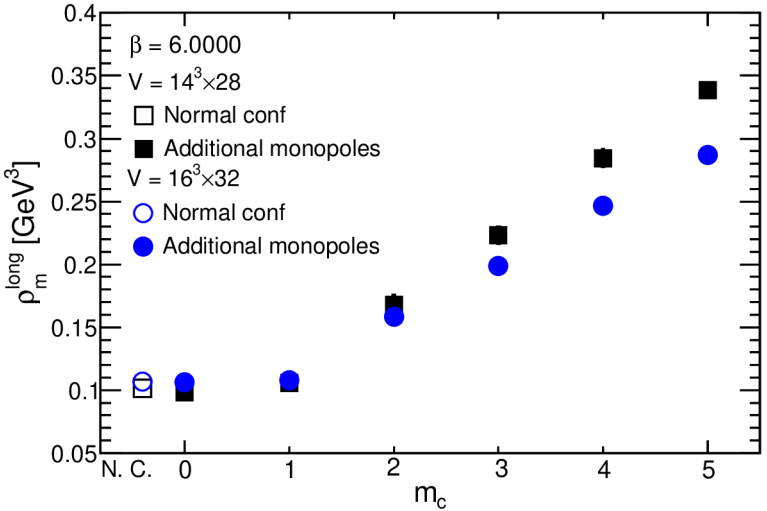

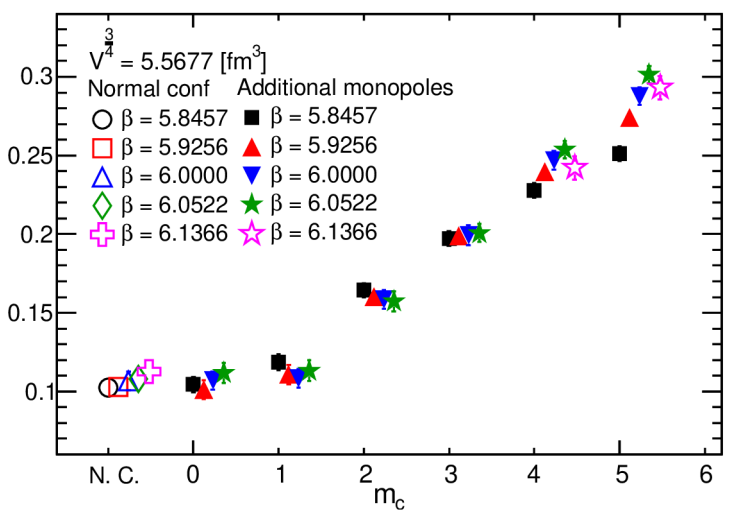

Color confinement and additional monopoles and dantimonopoles

At finite temperatures

- To reveal the effects of the additional monopoles and anti-monopoles on the phase transition of color deconfinement, we compute the Polyakov loop and determine the critical temperature.
- Polyakov loops: $P(\vec{x}) = \mathrm{Tr} \prod_{x_0=0}^{N_t-1} U(x,0)$
- Polyakov loop susceptibility:

$$\chi = V_s \left(\langle |P^2| \rangle - \langle |P| \rangle^2 \right)$$

- We fit a Gaussian function with 4 free parameters to determine $\mathbf{T_c}$.

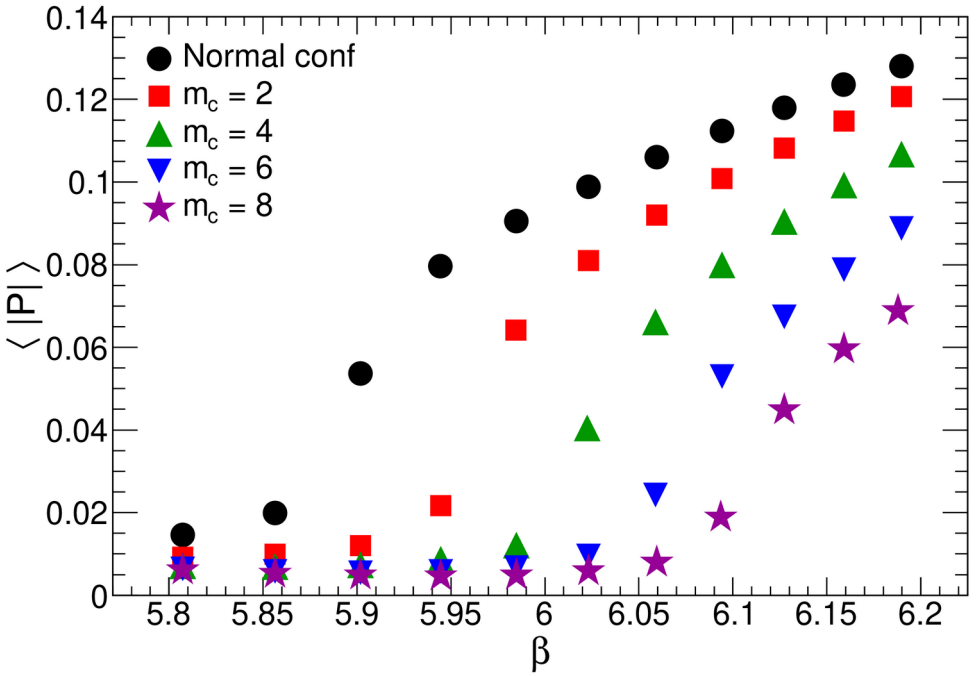

[arXiv: 2203.11357]

Color confinement and additional monopoles and anti-monopoles

- Comparisons with the Polyakov loops and the number density of the additional monopoles and anti-monopoles.

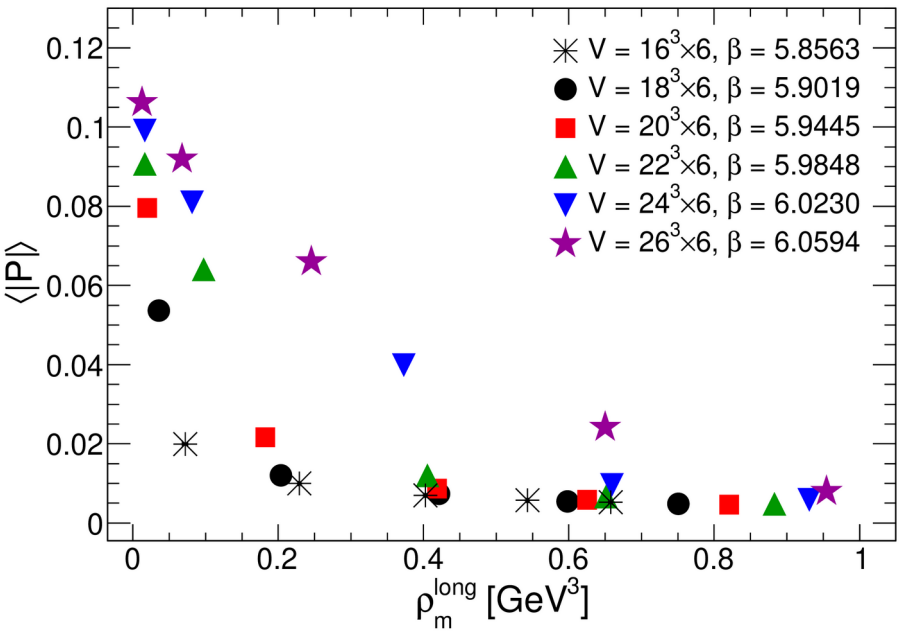

[arXiv: 2203.11357]

- Rising the critical temperature with the number of magnetic charges.

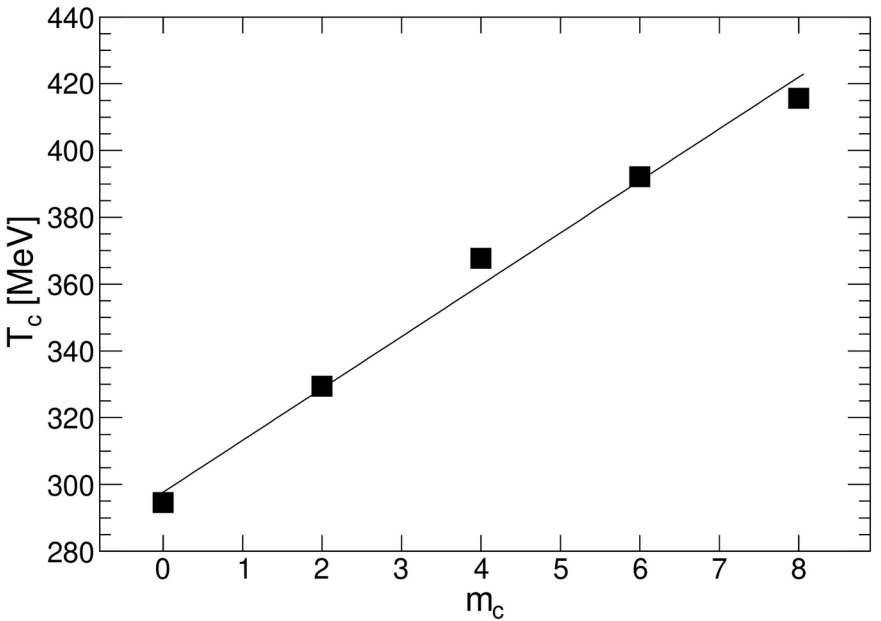

[arXiv: 2203.11357]

Overlap Dirac operator

- Chiral symmetry: $\mathcal{L} = \bar{\psi} D \psi$

$$\gamma_5 D + D \gamma_5 = 0$$

- The Dirac operator ***D***, which preserves the exact chiral symmetry in lattice gauge theory satisfies the following Ginsparg-Wilson relation [P. H. Ginsparg and K. G. Wilson PRD 25 (1982) 2649].

$$\gamma_5 \mathbf{D} + \mathbf{D} \gamma_5 = \mathbf{a D R} \gamma_5 \mathbf{D}$$

- The following **overlap Dirac operator *D*** satisfies the Ginsparg-Wilson relation [H. Neuberger, PLB 427 (1998) 353]:

$$D(\rho) = \frac{\rho}{a}\left[1 + \frac{D_W(\rho)}{\sqrt{D_W^\dagger(\rho) D_W(\rho)}}\right]$$

$$= \frac{\rho}{a}\{1 + \gamma_5 \epsilon(H_W(\rho))\}$$

- The sign function **ϵ** is approximated by the Chebyshev polynomials [Com. Phys. Comm. 153 (2003) 31].
- We solve the eigenvalue problems using ARPACK.

$$\mathbf{D}(\rho)|\psi_\mathbf{i}\rangle = \lambda_\mathbf{i}|\psi_\mathbf{i}\rangle$$

- We compute the pairs of eigenvalues $\boldsymbol{\lambda_i}$ and eigenvectors $|\psi_\mathbf{i}\rangle$ from the lowest energy level to approximately 100.

D: Massless overlap Dirac operater.

ϵ: Sign function.

$\mathbf{D_w}$: Massless Wilson Dirac operator.

ρ: Mass parameter **ρ = 1.4.**

$\boldsymbol{H_w}$: Hermitian Wilson Dirac operator.

Fermion zero modes and instantons

- **There are fermion zero modes in the eigenvalues of the overlap Dirac operator.**

  The number of **zero modes** of the **positive chirality is n_+.**

  The number of **zero modes** of the **negative chirality is n_-.**

- The exact zero modes λ_{Zero} are $|\lambda_{\mathbf{Zero}}| \leq \mathbf{O}(\mathbf{10^{-8}})$.
- We suppose that the Atiyah-Singer index theorem.

  The number of **instantons** of the **positive charge is n_+.**

  The number of **ant-instantons** of the **negative charge is n_-.**

- We have shown that the number of instantons and anti-instantons N_i can be calculated from the average square of the topological charges Q^2 [PRD 91 (2015) 054512]**:**

$$\mathbf{N_I} = \langle \mathbf{Q^2} \rangle, \ \mathbf{Q} = \mathbf{n_+} - \mathbf{n_-}$$

- **The number density of instantons and anti-instantons is**

$$\frac{N_I}{V} = \frac{\langle Q^2 \rangle}{V}$$

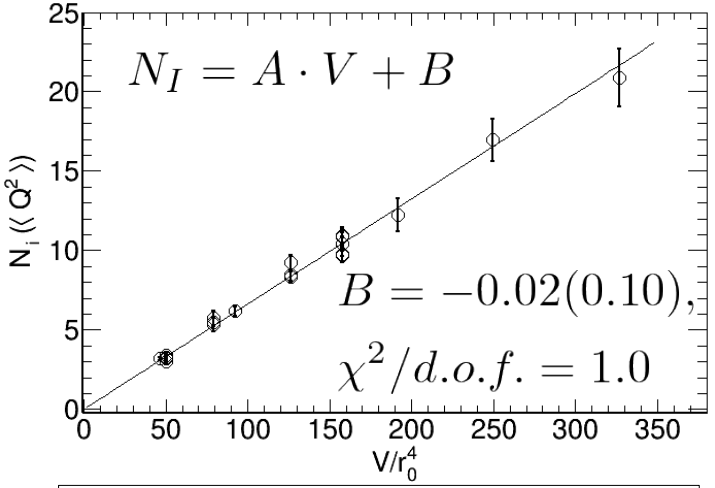

- **Instanton (anti-instanton) density**

$$\frac{Ar_0^4}{2} = \frac{N_I r_0^4}{2V}$$
$$= \mathbf{8.09(17)} \times \mathbf{10^{-4}} \ [\mathrm{GeV}^4]$$

- **E. V. Shuryak [NPB 203 (1982) 93]:**

$$\mathrm{n}_c = \mathbf{8} \times \mathbf{10^{-4}} \ [\mathrm{GeV}^4]$$

Monopoles and instantons

The quantitative relation between monopoles and instantons.

- We fit the following function.

$$N_I = Am_c + B$$

- The fitting results are

$$\mathbf{A} = \mathbf{1.23(13)},\ \mathbf{B} = \mathbf{10.7(4)},$$

$$\chi^2/d.o.f. = 2.9/5.0.$$

- The slope ***A*** is approximately **1**.
- The intercept of the prediction is the number of instantons and anti-instantons in V: $\boldsymbol{N_I^{Pre} = 10.414}$.

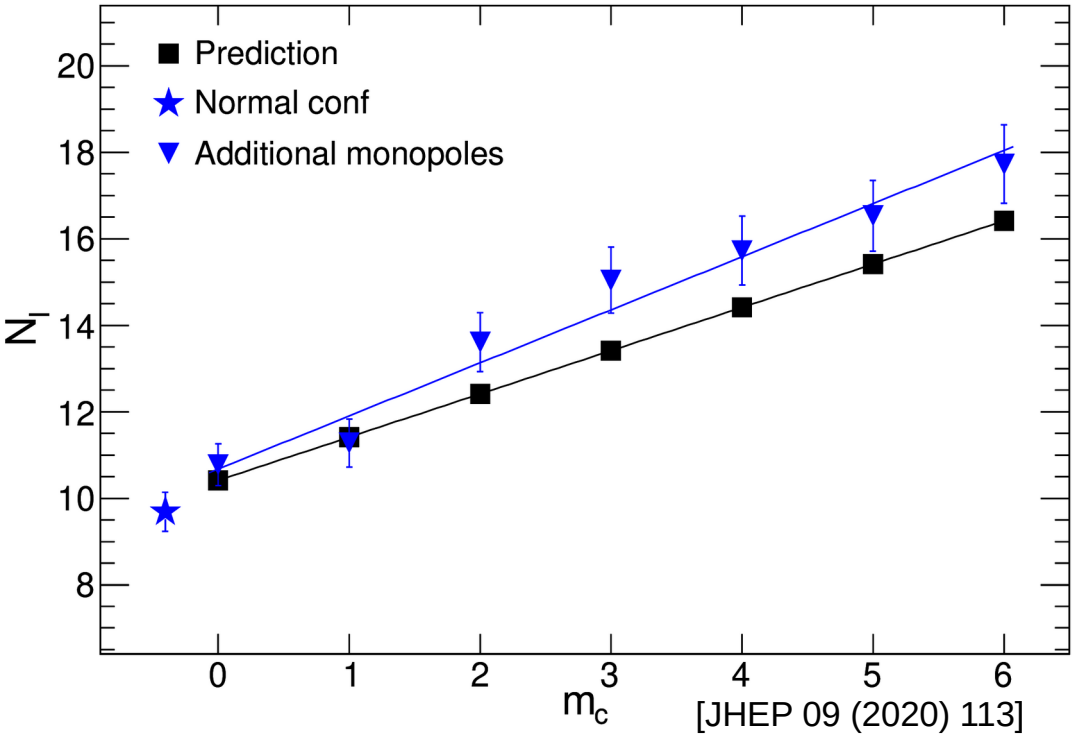

Monopoles and instantons

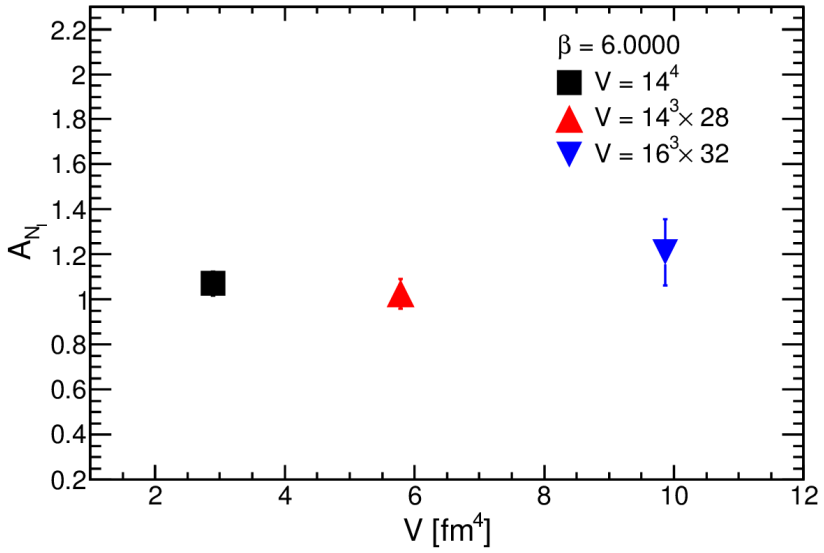

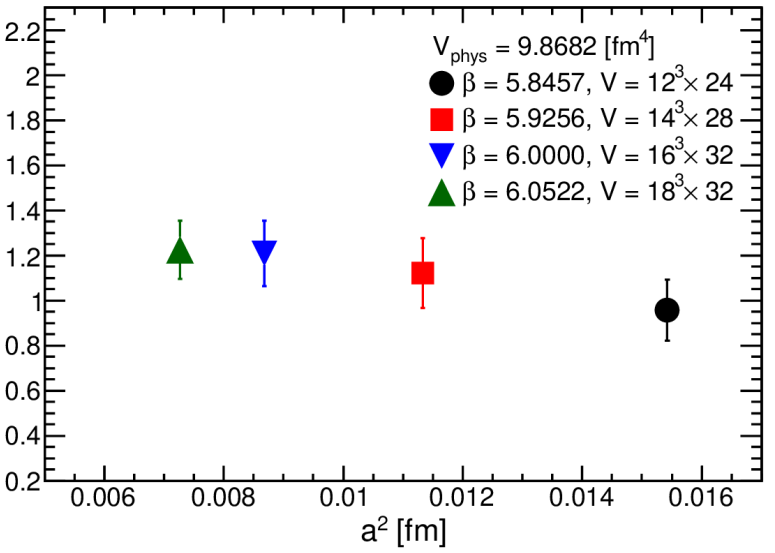

[arXiv: 2203.11357]

- **A monopole of magnetic charge +1 and an anti-monopole of magnetic charge -1 make one instanton or one anti-instanton** [PRD 91 (2015) 054512]**.**

Number density of the instantons and anti-instantons

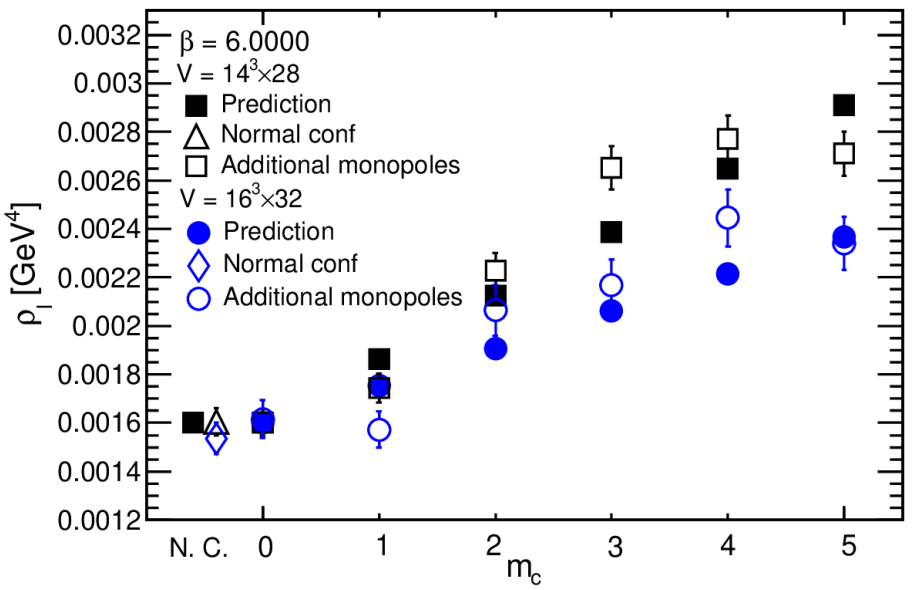

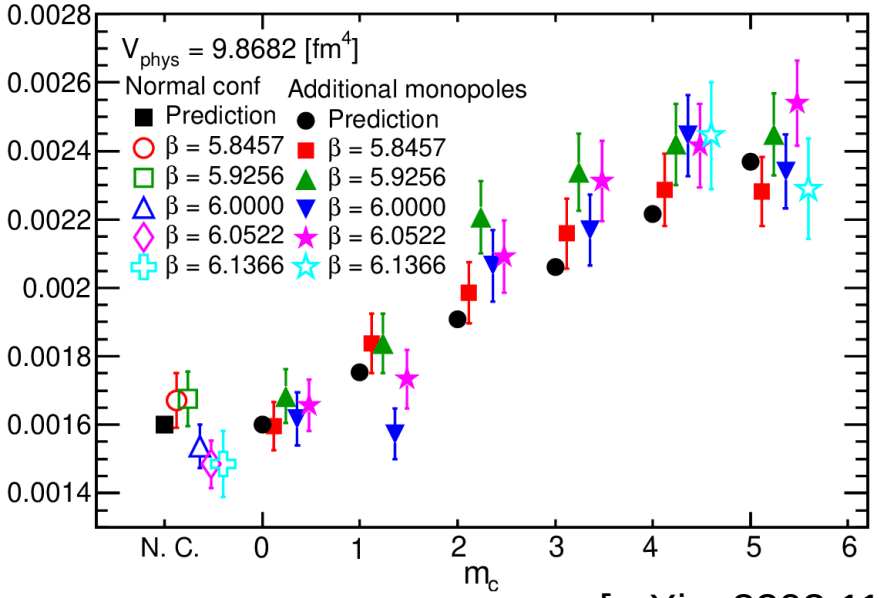

[arXiv: 2203.11357]

Making predictions

To quantitatively explain the decreases in the chiral condensate with increasing the monopole charges, we make the predictions.

- **Instanton vacuum**
  [Diakonov and Petrov, JTEP 62 (1985) 204]:

$$\langle\bar{\psi}\psi\rangle = -\frac{1}{\bar{\rho}}\left(\frac{\pi N_c}{13.2}\right)^{\frac{1}{2}}\left(\frac{N_I}{V}\right)^{\frac{1}{2}} = -(272.7\ [\mathrm{MeV}])^3.$$

- **The inverse of the average size of instanton**
  [NPB 203 (1982) 93]**:**

$$\frac{1}{\bar{\rho}} = 6.00\times 10^2\ \ [\mathrm{MeV}].$$

- **Gell-Mann-Oakes-Renner (GMOR) relation:**

$$\langle\bar{\psi}\psi\rangle = -\lim_{\bar{m}_q\to 0}\frac{(m_\pi F_\pi)^2}{2\bar{m}_q} = -(274^{+18}_{-8}\ [\mathrm{MeV}])^3.$$

- **Prediction of the chiral condensate:**

$$\langle\bar{\psi}\psi\rangle^{Pre} = -\frac{1}{\bar{\rho}}\left(\frac{\pi N_c}{13.2}\right)^{\frac{1}{2}}\left(\frac{N_I^{Pre}}{V}\right)^{\frac{1}{2}},$$

$$N_I^{Pre} = m_c + N_I^{Nor}.$$

- **Prediction of the decay constant at the chiral limit:**

$$F_0^{Pre} = \frac{1}{m_\pi}\left(\frac{2\bar{m}_q}{\bar{\rho}}\right)^{\frac{1}{2}}\left(\frac{\pi N_c}{13.2}\right)^{\frac{1}{4}}\left(\frac{N_I^{Pre}}{V}\right)^{\frac{1}{4}}.$$

- **For $m_c = 0$:**

$$F_0^{Pre} = 85^{+9}_{-4}\ [\mathrm{MeV}]$$

- **Chiral perturbation theory**
  [EPJC 33 (2004) 543]**:**

$$F_0^{\chi PT} = 86.2(5)\ [\mathrm{MeV}]$$

Operators and correlation functions

- **Quark propagator:**

$$G(\vec{y}, y^0; \vec{x}, x^0) \equiv \sum_i \frac{\psi_i(\vec{x}, x^0)\psi_i^\dagger(\vec{y}, y^0)}{\lambda_i^{mass}}$$

- λ_i^{mass} **of massive Dirac operator:**

$$\lambda_i^{mass} = \left(1 - \frac{a\bar{m}_q}{2\rho}\right)\lambda_i + \bar{m}_q$$

Light quark masses

- **Pion:** $\bar{m}_{ud} \equiv \dfrac{m_u + m_d}{2}$
- **Kaon:** $\bar{m}_{sud} \equiv \dfrac{m_s + \bar{m}_{ud}}{2}$

- **Scalar:** $\mathcal{O}_S = \bar{\psi}_1 \left(1 - \frac{a}{2\rho}D\right)\psi_2$
- **Pseudoscalar:** $\mathcal{O}_{PS} = \bar{\psi}_1\gamma_5 \left(1 - \frac{a}{2\rho}D\right)\psi_2$
- **Scalar density:**

$$C_{SS}(\Delta t) = \frac{a^3}{V}\sum_{\vec{x}_1}\sum_{\vec{x}_2,\ t}\langle \mathcal{O}_S^C(\vec{x}_2, t)\mathcal{O}_S(\vec{x}_1, t+\Delta t)\rangle$$

- **Pseudoscalar density:**

$$C_{PS}(\Delta t) = \frac{a^3}{V}\sum_{\vec{x}_1}\sum_{\vec{x}_2,\ t}\langle \mathcal{O}_{PS}^C(\vec{x}_2, t)\mathcal{O}_{PS}(\vec{x}_1, t+\Delta t)\rangle$$

- **Correlation function** [PRD 69 (2004) 074502]**:**

$$C_{PS-SS}(\Delta t) \equiv C_{PS}(\Delta t) - C_{SS}(\Delta t)$$

Fitting to the correlations

- We compute the correlations $C_{PS\text{-}SS}$ and aC_{AP}.
- The mass range of the bar quark is $a\bar{m}_q = 30 - 150$ [MeV].
- We determine two parameters $a^4G_{PS\text{-}SS}$ and am_{PS}, by fitting the following function:

$$C_{PS-SS}(t) = \frac{a^4 G_{PS-SS}}{am_{PS}} \exp\left(-\frac{m_{PS}}{2}T\right) \cosh\left[m_{PS}\left(\frac{T}{2} - t\right)\right].$$

- We set the fitting range so that the fitting result of χ^2/d.o.f. becomes approximately 1.
- We then calculate chiral condensate, light quark masses, meson masses, and decay constants using the fitting results $a^4G_{PS\text{-}SS}$ and am_{PS}.

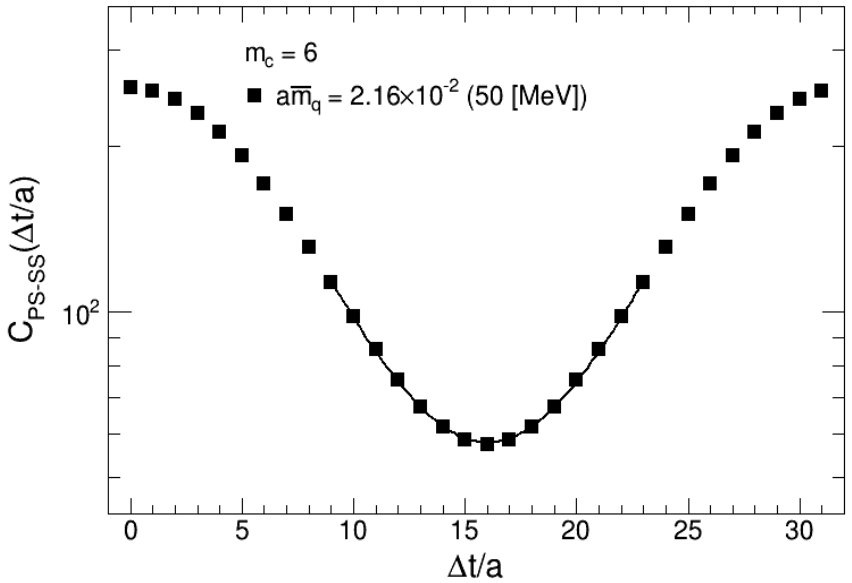

Fitting result:

χ^2/d.o.f. ≈ 0.6 (FR Δt/a = 9-23).

PCAC relation

- We check the effects of the added monopoles and anti-monopoles and created instantons and anti-instantons on the following PCAC relation.

$$\mathbf{m_{PS}^2 = A\bar{m}_q}$$

- To quantitatively evaluate the effects, we fit the following functions to the numerical results.

$$(am_{PS})^2 = \mathbf{aA^{(1)}}a\bar{m}_q + a^2B$$

$$(am_{PS})^2 = \mathbf{aA^{(2)}}a\bar{m}_q$$

- The added monopoles and anti-monopoles and created instantons and anti-instantons do not affect the PCAC relation.
- We compute physical quantities using the fitting results of slope $a\boldsymbol{A}^{(2)}$.

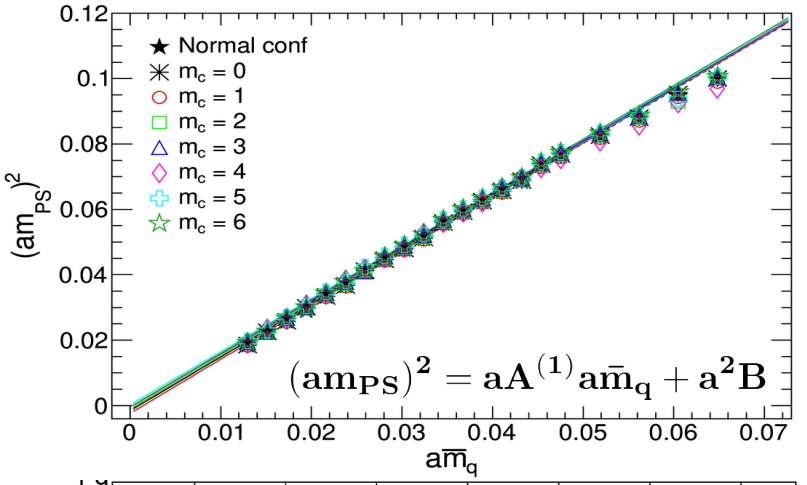

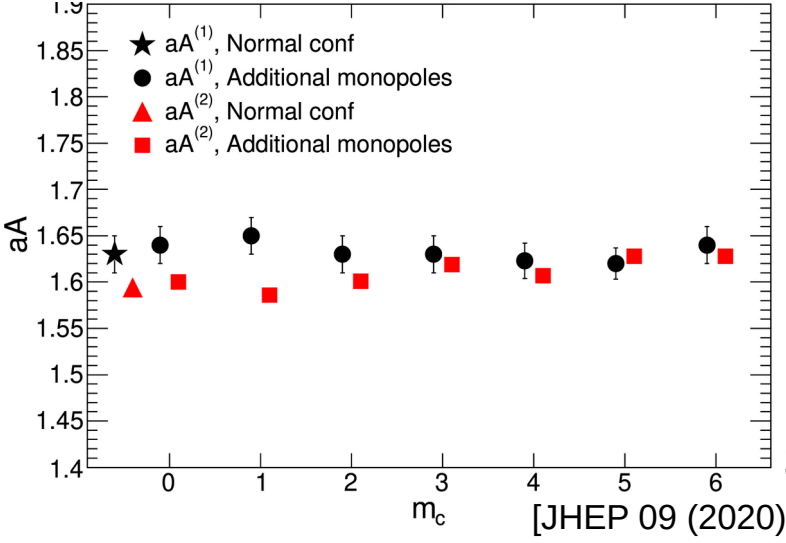

[JHEP 09 (2020) 113]

Instanton effects

To compare the numerical results with the experimental results, we improve the determination method of the lattice spacing in references [NPB 489 (1997) 427, PRD 64 (2001) 114508]**.**

- We set the scale of the lattice so that it is analytically calculated.
- We match the numerical results of the decay constant and the square of the mass with the experimental results of the pion and kaon and determine the **normalization factors Z_π and Z_K**.
- We then evaluate the decay constants and the chiral condensate using the normalization factors.
- We evaluate the instanton effects on the masses of the light quarks and mesons and the decay constants of the mesons.
- Finally, we estimate the catalytic effect on the charged pion.

Matching with experiments

Determining the normalization factors by matching the numerical results with the experimental results of pion and kaon.

- Fitting function: $aF_{PS} = a^{-1}A(am_{PS})^2 + aB.$
- We make two functions as follows:
  - **Pion**:
    $$aF_{PS} = C_{\pi}^{Exp.} am_{PS},\ C_{\pi}^{Exp.} = \frac{F_{\pi^-}^{Exp.}}{\sqrt{2}m_{\pi^\pm}^{Exp.}} = \frac{92.277}{139.570}.$$
  - **Kaon**:
    $$aF_{PS} = C_{K}^{Exp.} am_{PS},\ C_{K}^{Exp.} = \frac{F_{K^-}^{Exp.}}{\sqrt{2}m_{K^\pm}^{Exp.}} = \frac{110.11}{493.677}.$$
- We calculate the intersections between these functions (normal conf).
  - **Pion**: $(aF_{PS}^{\pi}, am_{PS}^{\pi}) = (3.13(6), 4.74(8) \times 10^{-2}).$
  - **Kaon**: $(aF_{PS}^{K}, am_{PS}^{K}) = (3.80(10), 0.171(4)).$

[JHEP 09 (2020) 113]

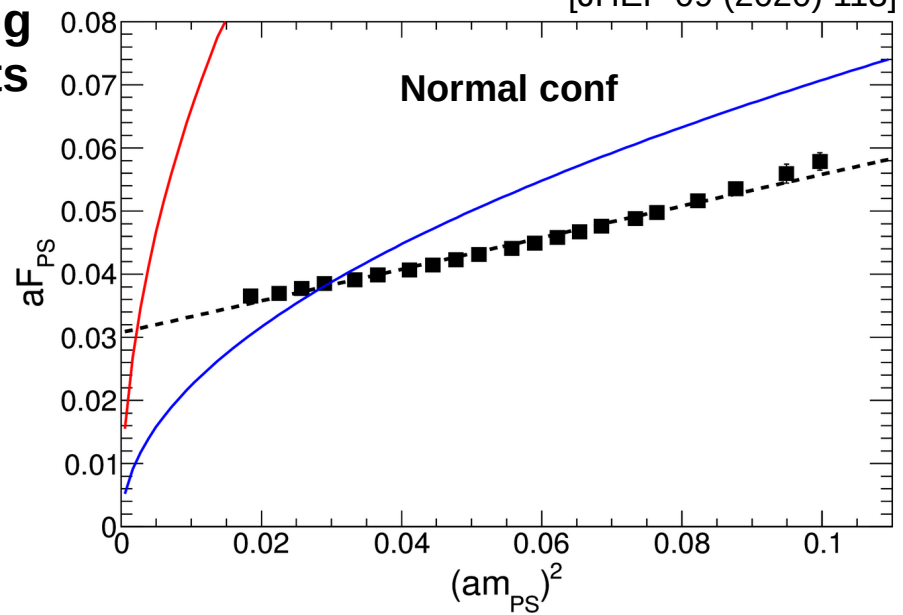

- **Normalization factors:**

$$Z_{\pi} = \frac{F_{\pi^-}^{Exp.}}{\sqrt{2}F_{PS}^{\pi}} = \frac{m_{\pi^\pm}^{Exp.}}{m_{PS}^{\pi}} = 1.27(2)$$

$$Z_{K} = \frac{F_{K^-}^{Exp.}}{\sqrt{2}F_{PS}^{K}} = \frac{m_{K^\pm}^{Exp.}}{m_{PS}^{K}} = 1.25(3)_{33}$$

Matching with experiments

Determining the normalization factors by matching the numerical results with the experimental results of pion and kaon.

- Fitting function: $aF_{PS} = a^{-1}A(am_{PS})^2 + aB.$
- We make two functions as follows:
  - **Pion**:

$$aF_{PS} = C_{\pi}^{Exp.} am_{PS},\ C_{\pi}^{Exp.} = \frac{F_{\pi^-}^{Exp.}}{\sqrt{2}m_{\pi^\pm}^{Exp.}} = \frac{92.277}{139.570}.$$

  - **Kaon**:

$$aF_{PS} = C_{K}^{Exp.} am_{PS},\ C_{K}^{Exp.} = \frac{F_{K^-}^{Exp.}}{\sqrt{2}m_{K^\pm}^{Exp.}} = \frac{110.11}{493.677}.$$

- We calculate the intersections between these functions for each magnetic charge.

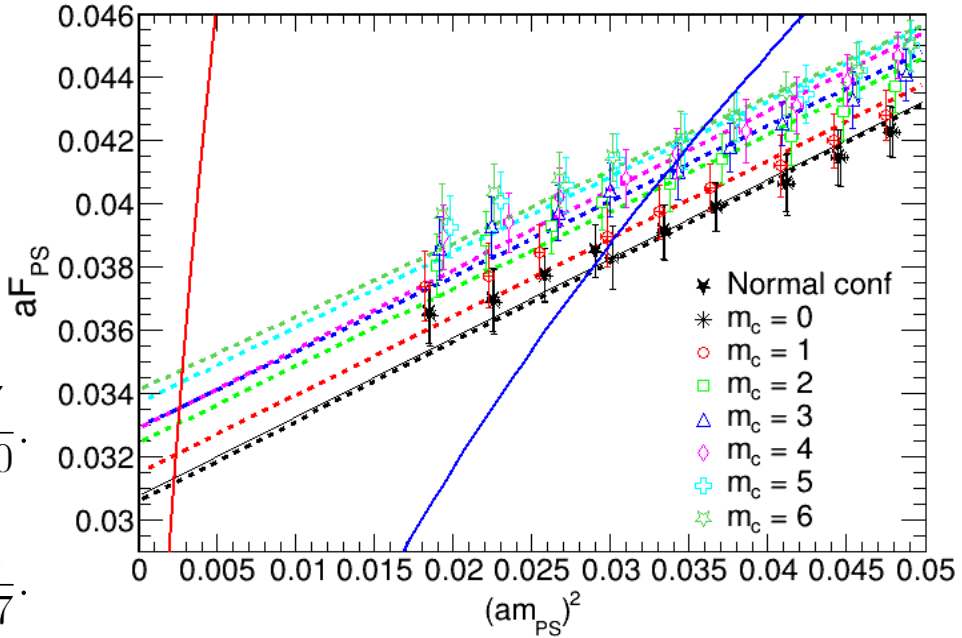

- **Normalization factors:**

$$Z_\pi = \frac{F_{\pi^-}^{Exp.}}{\sqrt{2}F_{PS}^{\pi}} = \frac{m_{\pi^\pm}^{Exp.}}{m_{PS}^{\pi}} = 1.27(2)$$

$$Z_K = \frac{F_{K^-}^{Exp.}}{\sqrt{2}F_{PS}^{K}} = \frac{m_{K^\pm}^{Exp.}}{m_{PS}^{K}} = 1.25(3)_{34}$$

Instanton effects on chiral condensate

[arXiv: 2203.11357]

- The chiral condensate is derived using the slope $aA^{(2)}$ of the PCAC relation and the decay constant F_0^Z.

$$a^3\langle\bar{\psi}\psi\rangle^Z = -\frac{aA^{(2)}}{2}(aF_0^Z)^2,\ (F_0^Z = Z_\pi F_0).$$

- The renormalized chiral condensate in the MS-bar scheme at 2 [GeV]:

$$\langle\bar{\psi}\psi\rangle^Z_{\overline{MS}} = \frac{\hat{Z}_S}{0.72076}\langle\bar{\psi}\psi\rangle^Z$$

- The fitting curve:

$$\langle\bar{\psi}\psi\rangle = -A_\chi\left(\frac{N_I}{V}\right)^{\frac{1}{2}}$$

- Fitting results (interpolated results):

$$A_\chi = 0.484(6)\ [\mathrm{GeV}], \chi^2/d.o.f. = 1.0/6.0.$$

$$A_\chi^{Pre} = 0.5070\ [\mathrm{GeV}]$$

- Inverse of average size of instanton:

$$\frac{1}{\bar{\rho}} = 5.73(7)\times 10^2\ [\mathrm{MeV}].$$

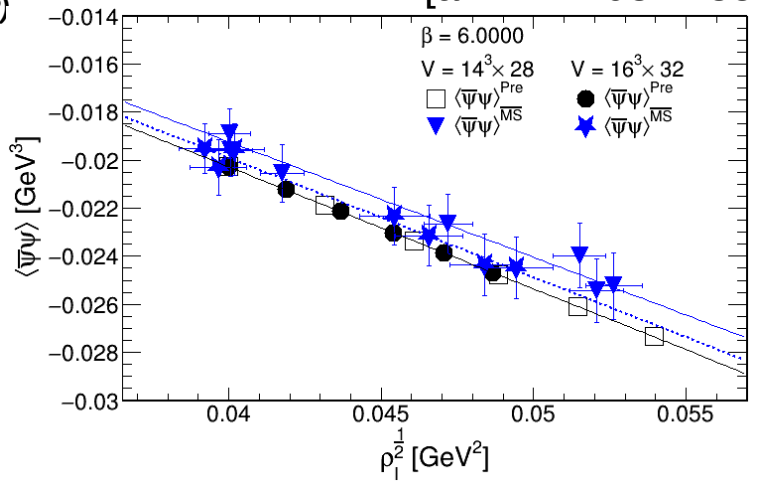

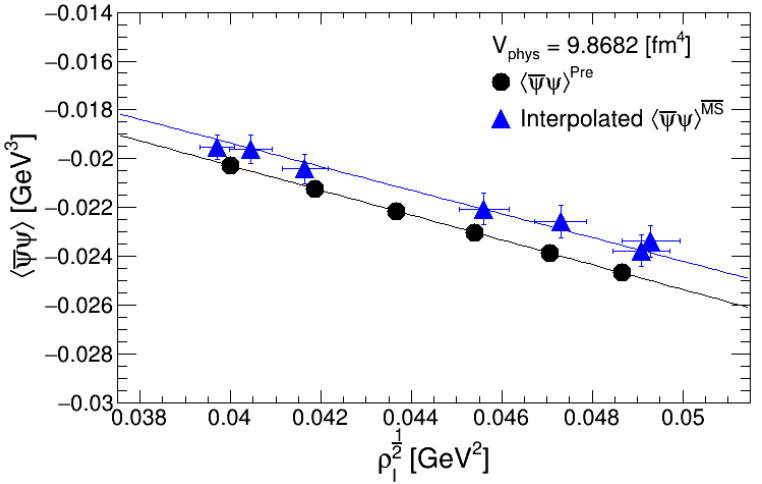

Instanton effects on quark masses

We evaluate the renormalized light quark masses in the MS-bar scheme at 2 [GeV] using calculated intersection results at the masses and decay constants of the pion and kaon, $aA^{(2)}$, Z_π, and Z_K.

- The average mass of u and d quarks:

$$a\bar{m}_{ud}^{Z} = \frac{(Z_\pi a m_{PS}^{\pi})^2}{aA^{(2)}}.$$

- The average mass of u, d, and s quarks:

$$a\bar{m}_{sud}^{Z} = \frac{am_s^Z + a\bar{m}_{ud}^Z}{2} = \frac{(Z_K a m_{PS}^{K})^2}{aA^{(2)}}.$$

- The strange quark mass:

$$am_s^Z = \frac{2(Z_K a m_{PS}^{K})^2 - (Z_\pi a m_{PS}^{\pi})^2}{aA^{(2)}}.$$

- Renormalized quark masses in the MS-bar scheme at 2 [GeV] (Z_s is normal conf,):

$$\hat{m}_q^{\overline{MS}} = \frac{0.72076}{Z_S} m_q^Z,$$
$$(m_q^Z = \bar{m}_{ud}^Z,\ \bar{m}_{sud}^Z,\ m_s^Z).$$

- Numerical results of renormalized quark masses of the normal configurations:

$$\hat{\bar{m}}_{ud}^{\overline{MS}}\ (2\ [\mathrm{GeV}]) = 4.09(10)\ [\mathrm{MeV}],$$
$$\hat{m}_s^{\overline{MS}}\ (2\ [\mathrm{GeV}]) = 98(3)\ [\mathrm{MeV}].$$

- The experimental results:

$$\bar{m}_{ud}^{Exp.} = 3.5^{+0.7}_{-0.3}\ [\mathrm{MeV}],$$
$$m_s^{Exp.} = 96^{+8}_{-4}\ [\mathrm{MeV}].$$

Instanton effects on quark mass

- We derive the prediction regarding the light quark masses from the experimental results as follows:

$$\bar{m}_{ud}^{\mathrm{Pre}}(m_c) = \bar{m}_{ud}^{\mathrm{Exp}} \left[\frac{\rho_I^{\mathrm{Pre}}(m_c)}{\rho_I^{\mathrm{sta}}} \right]^{\frac{1}{2}}$$

[arXiv: 2203.11357]

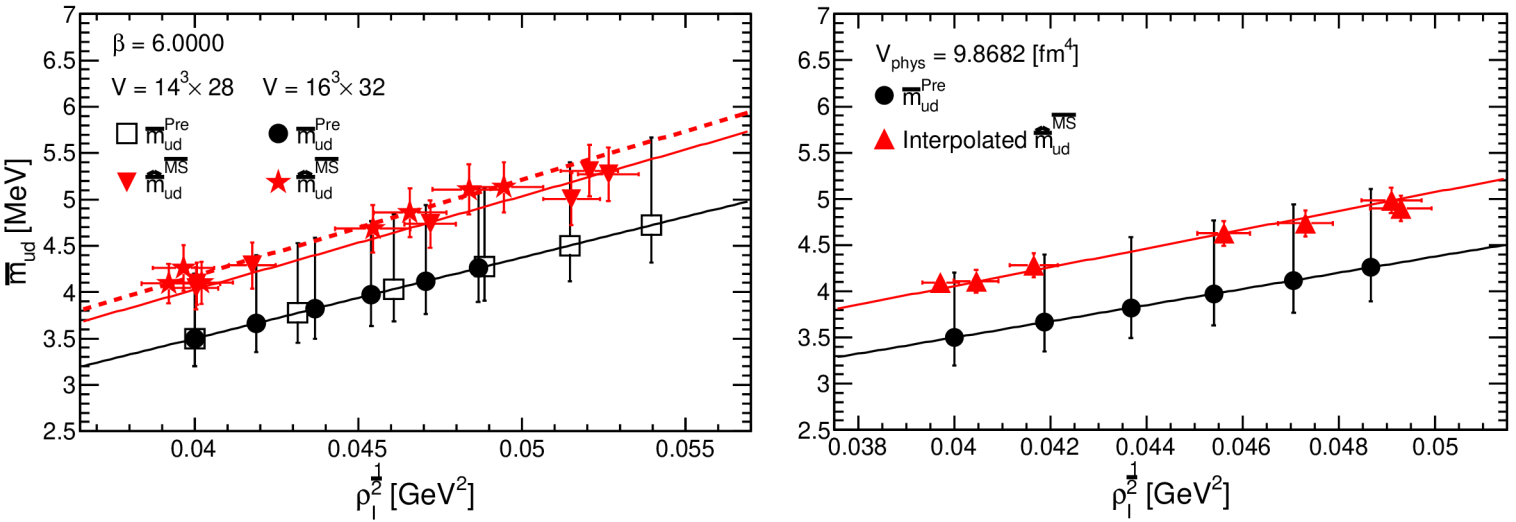

- The slopes of the fitting results are reasonably consistent with the predictions.
- The light quark masses increase in **direct proportion** to the **square root** of the number density of the instantons and anti-instantons.

Instanton effects on pion mass

- From the PCAC relation, the pion and kaon masses increase in direct proportion to the one-fourth root of the number density of the instantons and anti-instantons.
- The prediction of the pion mass using the experimental results is as follows:

$$m_{\pi}^{\mathrm{Pre}}(m_c) = m_{\pi^{\pm}}^{\mathrm{Exp}} \left[\frac{\rho_I^{\mathrm{Pre}}(m_c)}{\rho_I^{\mathrm{sta}}} \right]^{\frac{1}{4}}$$

[arXiv: 2203.11357]

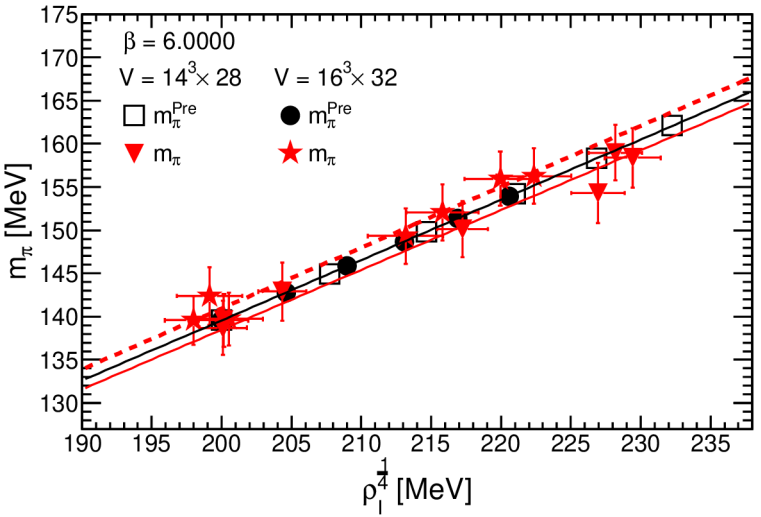

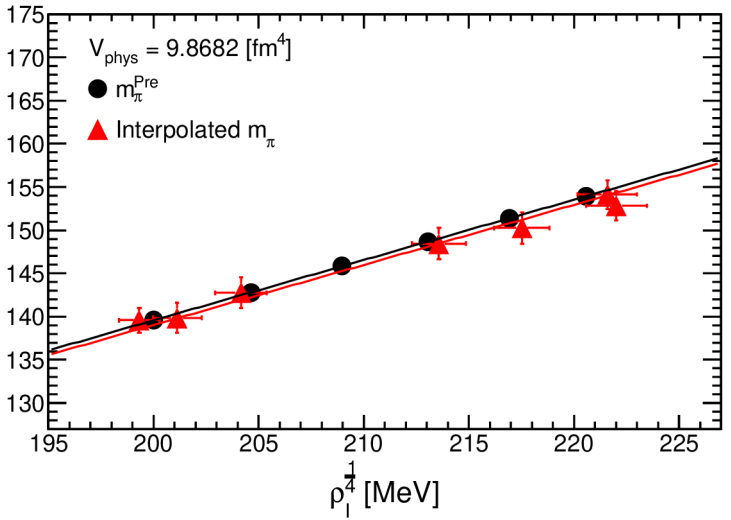

- The pion and kaon masses increase in **direct proportion** to the **one-fourth root** of the number density of the instantons and anti-instantons.

Instanton effects on pion decay

- The formula in the quenched chiral perturbation theory in SU(2) holds; therefore, the decay constants of pion and kaon are in direct proportion to the one-fourth root of the number density of the instantons and anti-instantons.
- Prediction for pion: $$F_\pi^{\mathrm{Pre}}(m_c) = \frac{F_{\pi^-}^{\mathrm{Exp}}}{\sqrt{2}} \left[\frac{\rho_I^{\mathrm{Pre}}(m_c)}{\rho_I^{\mathrm{sta}}} \right]^{\frac{1}{4}}$$ [arXiv: 2203.11357]

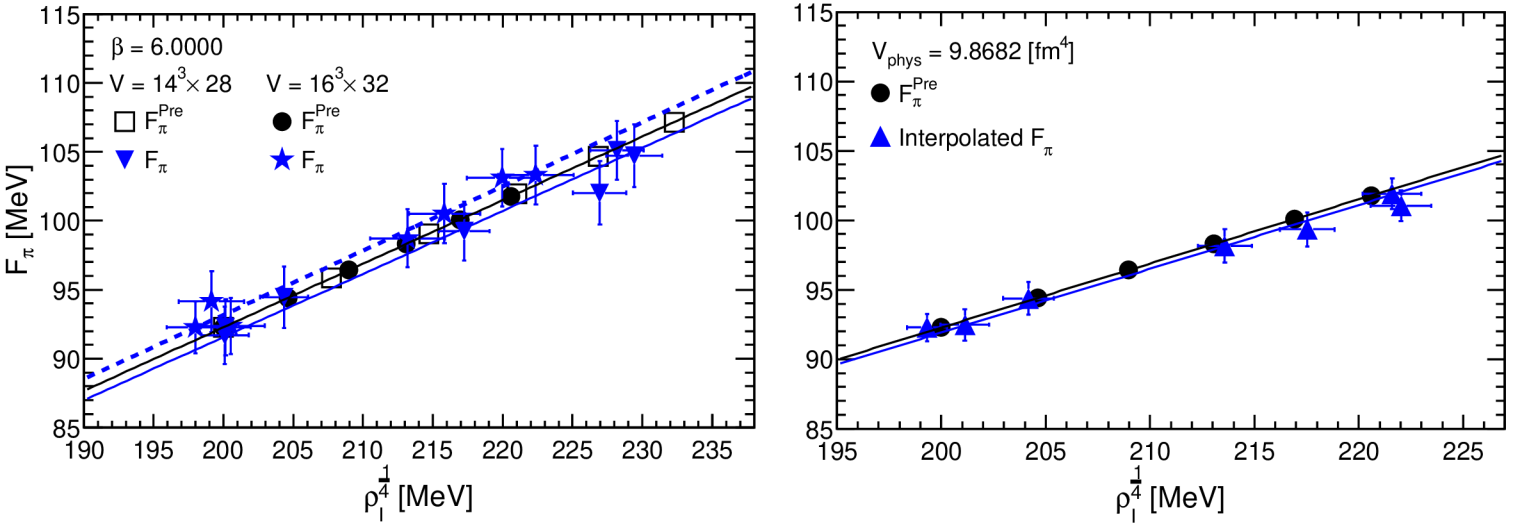

- The pion decay constant increases in **direct proportion** to the **one-fourth root** of the number density of the instantons and anti-instantons.

Catalytic effect on the pion decay

- One charged pion decays to a lepton (an electron or a muon) and a neutrino as follows:

$$\pi^+ \to l^+ + \nu_l, \quad \pi^- \to l^- + \bar{\nu}_l$$

- These decays are induced by the weak interaction, and the decay width of the charged pion is derived [text book, T. Kugo] as follows:

$$\Gamma(\pi^- \to l + \bar{\nu}_l) = \frac{(G_F F_\pi \cos\theta_c)^2}{4\pi m_\pi^3} m_l^2 (m_\pi^2 - m_l^2)^2.$$

- We estimate the total decay width of the charged pion from the partial decay width, where the charged pion decays to the muon. The lifetime is estimated as follows:

$$\tau = \frac{1}{\Gamma(\pi^- \to \mu + \bar{\nu}_\mu)}.$$

- We substitute the numerical results of the mass and decay constant of pion and their predictions for these formulas and estimate the catalytic effect on the charged pion.
- Finally, to quantitatively evaluate the catalytic effect, we fit the following curves:

$$y(x) = p_1 x^3 - p_2 x + \frac{p_3}{x}, \text{or } y(x)^{-1}, \; x = \left(\frac{N_I}{V}\right)^{\frac{1}{4}}$$

Decay width on the charged pion

[arXiv: 2203.11357]

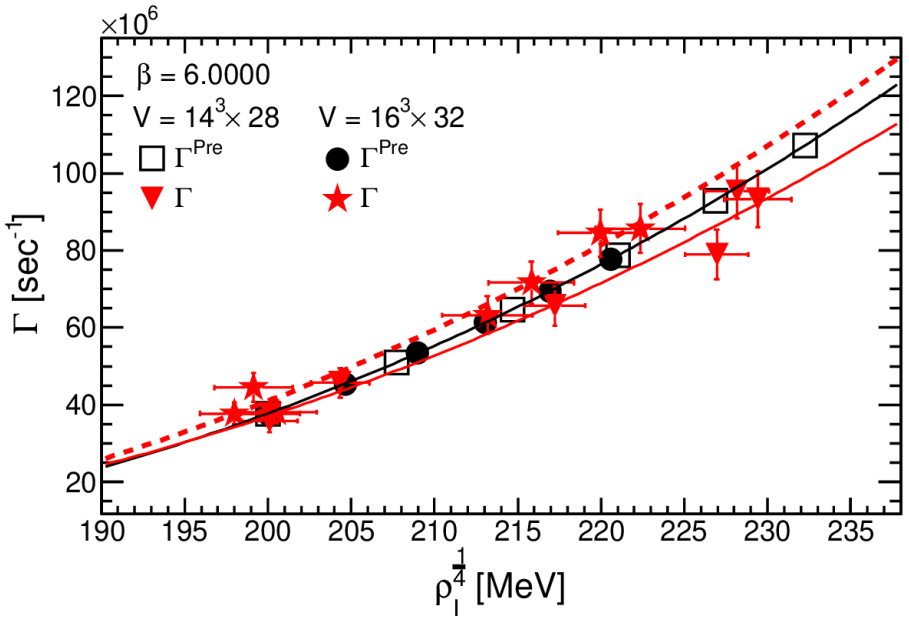

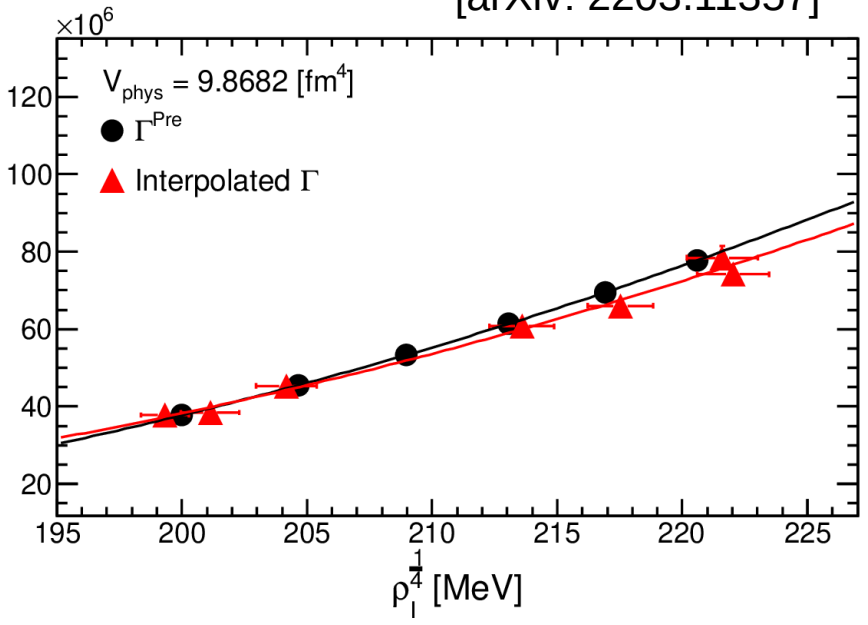

- The decay width of the charged pion becomes wider than the experimental result by increasing the number density of the instantons and anti-instantons.

Catalytic effect on the charged pion

[arXiv: 2203.11357]

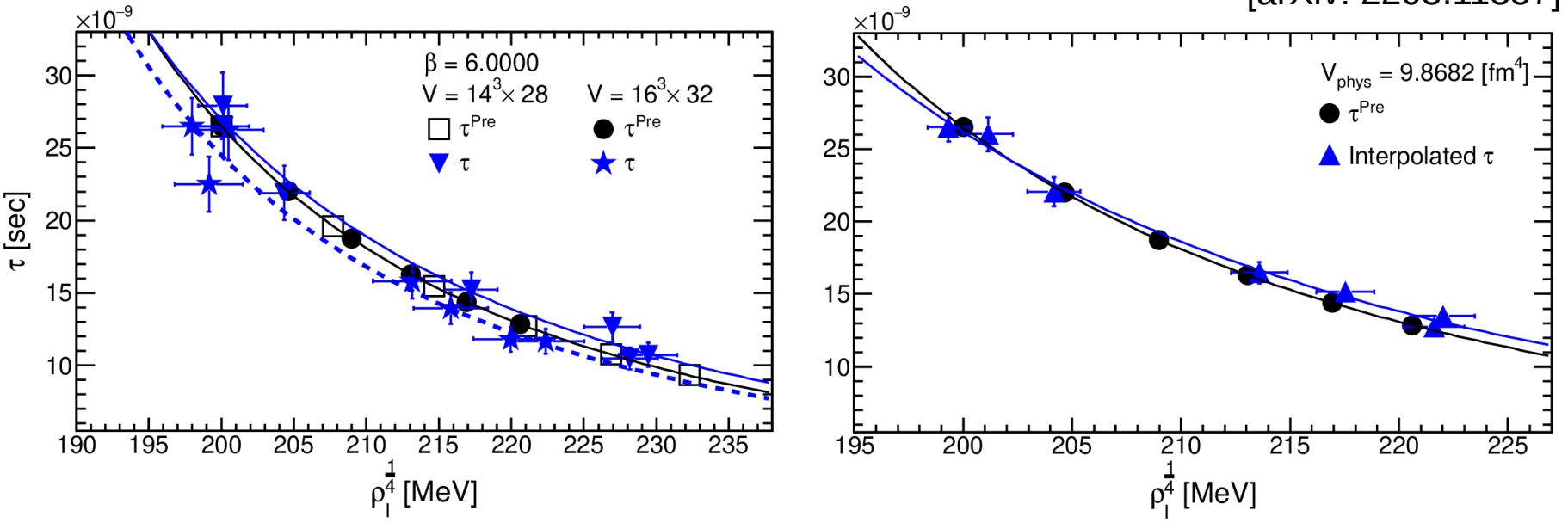

- The lifetime of the charged pion becomes shorter than the experimental outcome by increasing the number density of the instantons and anti-instantons.
- **This is the catalytic effect of monopole and instanton creation.**

Conclusions

- The monopole creation operator makes only the long monopole loops, which are the crucial elements for the mechanism of color confinement.
- The critical temperature rises by increasing the magnetic charges of the monopoles and anti-monopoles.
- A monopole with magnetic charge $\boldsymbol{m_c = 1}$ and an anti-monopole with magnetic charge $\boldsymbol{m_c = -1}$ produce one instanton or one anti-instanton.
- The monopole creation operator creates the topological charges without affecting the vacuum structure.
- The distributions of the nearest-neighbor spacing and the spectral rigidity correspond perfectly with the results of the GUE in the GRMT, even if we add the monopoles and anti-monopoles.
- The ratios of the low-lying eigenvalues and the distributions of the first eigenvalues of each topological sector agree with the results of the GUE in the chRMT.
- The additional monopoles and anti-monopoles do not affect the eigenvalues and change only the scale parameter $\boldsymbol{\Sigma}$ of the eigenvalue distribution.

Conclusions

- The chiral condensate, which is calculated from the scale parameter, decreases when increasing the magnetic charges.
- The values of the chiral condensate decrease in direct proportion to the **square root** of the number density of the instantons and anti-instantons.
- The decay constant of the pseudoscalar at the chiral limit increases in direct proportion to the **one-fourth root** of the number density of the instantons and anti-instantons.
- The average mass of u and d quarks increases in direct proportion to the **square root** of the number density of the instantons and anti-instantons.
- The mass and decay constant of the pion increase in direct proportion to the **one-fourth root** of the number density of the instantons and anti-instantons.
- The decay width of the charged pion becomes wider than the experimental result by increasing the number density of the instantons and anti-instantons.
- The lifetime of the charged pion becomes shorter by increasing the number density of the instantons and anti-instantons.

Acknowledgments

- I performed simulations using supercomputers (SX-series, OCTOPUS, SQUID, SR, XC40) and PC-clusters at the Research Center for Nuclear Physics (RCNP) and Cybermedia Center (CMC) at Osaka University and the Yukawa Institute for Theoretical Physics at Kyoto University.
- I use the storage elements of the Japan Lattice Data Grid at the RCNP.
- I appreciate the computer resources and technical support that these facilities provided for this project.